Research Article

For reprint orders, please contact: reprints@futuremedicine.com

Epigenomics

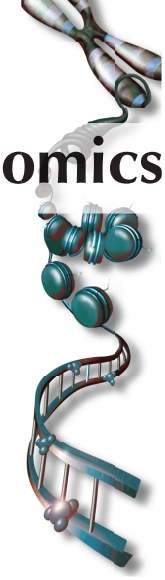

Sex-specific epigenetic mediators between early life social disadvantage and adulthood BMI

Su H Chu[1,2], Eric B Loucks[1], Karl T Kelsey[1,3], Stephen E Gilman[4,5,6,7], Golareh Agha[8], Charles B Eaton[1,9], Stephen L Buka[1] & Yen-Tsung Huang*[,1,10,11]

[1]Department of Epidemiology, Brown School of Public Health, Providence, RI, 02912, USA
[2]Channing Division of Network Medicine, Brigham & Women's Hospital & Harvard Medical School, Boston, MA, 02115, USA
[3]Department of Pathology & Laboratory Medicine, Brown University Warren Alpert Medical School, Providence, RI, 02912, USA
[4]Health Behavior Branch, Division of Intramural Population Health Research, Eunice Kennedy Shriver National Institute of Child Health & Human Development, Bethesda, MD, 20892, USA
[5]Department of Social & Behavioral Sciences, Harvard TH Chan School of Public Health, Boston, MA, 02115, USA
[6]Department of Epidemiology, Harvard TH Chan School of Public Health, Boston, MA, 02115, USA
[7]Department of Mental Health, Johns Hopkins Bloomberg School of Public Health, Baltimore, MD, 21205, USA
[8]Columbia Aging Center, Mailman School of Public Health, Columbia University, New York, NY, 10032, USA
[9]Department of Family Medicine, Brown University Warren Alpert Medical School, Providence, RI, 02912, USA
[10]Department of Biostatistics, Brown School of Public Health, Providence, RI, 02912, USA
[11]Institute of Statistical Science, Academia Sinica, Taipei, 11529, Taiwan
*Author for correspondence: ythuang@stat.sinica.edu.tw

Aim: The objective of this study was to identify potential epigenetic mediating pathways linking early life social disadvantage (ELSD) to adulthood BMI. **Methods:** Sex-specific epigenome-wide two-stage mediation analyses were conducted in blood and adipose tissue, and mediation estimates were obtained using cross-product mediation analysis. Pathway analyses were conducted using GREAT software (Bejerano Lab, CA, USA). **Results:** Candidate mediation CpG sites were identified in adipose tissue, but not blood, and were sex-specific. Significant mediation sites in females included CpG loci in genes: *PKHG1*, *BCAR3*, *ADAM5P*, *PIEZO1*, *FGFRL1*, *FASN* and *DPP9*, among others. Pathway analyses revealed evidence of enrichment for processes associated with *TFG-β* signaling and immunologic signatures. In males, significant mediation loci included sites in *MAP3K5* and *RPTOR*, which have previously been associated with adipogenesis, inflammation and insulin resistance. **Conclusion:** Our findings provide supportive evidence for the mediating role of epigenetic mechanisms in the effect of early life social disadvantage on adulthood BMI.

First draft submitted: 30 October 2017; Accepted for publication: 9 January 2018; Published online: 11 June 2018

Keywords: adipose tissue • adiposity • BMI • childhood adversity • DNA methylation • epigenetics • social disadvantage • social epidemiology

Epigenetic pathways, such as altered DNA methylation (DNAm), have been hypothesized as plausible mechanisms by which early life exposures and adult disease may be linked [1–4]. Evidence for the association between childhood social environments and epigenetic programming within genes related to stress reactivity and inflammation continues to grow [5–9]. Furthermore, as evidence for the ability of early life social environments to effect change on epigenetic pathways has increased, so too has the evidence for dysregulation of epigenetic processes in adiposity [10–14], suggesting a possible connection between social adversity and obesity vis-à-vis epigenetic mediators.

Few studies have directly interrogated the mediating role of epigenetic mechanisms in the impact of early life social disadvantage (ELSD) on adulthood adiposity. A previous mediation study identified sex-specific methylation loci in biologically plausible genes that were strong mediation candidates for the effect of childhood socioeconomic status (SES) on adulthood BMI in adipose tissue [15]. However, childhood SES does not explicitly include psychosocial or environmental measures of social disadvantage. Indeed, social adversity in the form of adverse childhood experiences has been shown to associate with adiposity independently of SES [16–22]. To this end, we conducted mediation

Future Medicine

analyses in biologically relevant adipose tissue to formally assess potential alterations in DNAm that might lie on the pathway between ELSD and adulthood adiposity. Given accumulating evidence of differential methylation patterns [15–17] as well as differential effects of socioeconomic factors on adiposity between males and females [15,18], mediation analyses were stratified by sex. As both psychosocial and environmental exposures have also been shown to associate with adiposity, we reasoned that an inclusive measure extending beyond only socioeconomic status would provide a more accurate and holistic measure of early life experiences. Thus, ELSD was conceived as a composite index of not only socioeconomic but also specific environmental and psychosocial measures of adversity. The objective of this study was to identify epigenetic-mediating mechanisms through which ELSD could influence adulthood BMI, utilizing a prospective study with directly assessed ELSD during childhood, as well as BMI and epigenetic methylation patterns in blood and adipose tissue during middle adulthood.

Materials & methods

Study sample

Study participants were recruited from the Longitudinal Effects on Aging Perinatal (LEAP) Project, a nested substudy of the New England Family Study (NEFS). The NEFS is a large prospectively assessed cohort of 17,921 offspring of pregnant women in the Collaborative Perinatal Project who were born in Providence, Rhode Island and Boston, MA (USA) between 1959 and 1966. The LEAP substudy enrolled and assessed 400 Providence-born participants who were not deceased, not incarcerated, had assessments taken at age 7 years, and were located within 100 miles of a clinical assessment site during 2010–2011. Of these, 316 had adequate adipose tissue biopsy performed, 68 refused adipose tissue biopsies and 16 had inadequate biopsy specimens. A final, representative sample of 143 of these 316 participants was selected for blood and adipose tissue methylation analyses. The study protocol was approved by the institutional review boards at Brown University and Memorial Hospital of Rhode Island.

Collection of covariates & tissue samples

Bodyweight and height were obtained by trained personnel using a calibrated stadiometer and weighing scale, and then converted into BMI as weight per height squared (kg/m^2). ELSD was assessed prospectively at age 7 using a composite summary score by summing across ten component measures of social disadvantage (Gilman et al., Submitted). For each component measure, a score of 0 (low adversity), 0.5 (medium adversity) or 1 (high adversity) was assigned. The components comprising the summary score were: parental income (>150% poverty threshold, 100–150% poverty threshold, <poverty threshold); parental occupation (nonmanual, manual, welfare only); household crowding (<1 person/room, 1–1.5 persons/room, ≥1.5 persons/room); family structure (two parents at home, single parent, divorced or separated); changes in parent's marital status (0, 1, 2+); number of moves since birth (0–1, 2, 3+); parental employment history (employed, not employed in the past year, 1+ years unemployed); changes in primary caregiver (no, yes); death of a sibling (no, yes); and age 7 change in economic situation since birth (same or better, worse). All possible component category options above were presented from low to high adversity. Changes in primary caregiver, death of a sibling and change in economic situation since birth are binary covariates and thus were classified as either low or high. A maximum score of ten was possible. Other covariates of interest included age at time of clinical assessment, race (white or nonwhite), sex, prenatal maternal smoking (cigarettes/day) and BMI at age 7.

Tissue sample collection & methylation profiling

Subcutaneous adipose tissue samples were aspirated from the upper outer quadrant of the buttock via 16-gauge needle. Whole blood samples were centrifuged to obtain buffy coat. DNA extraction from the adipose tissue samples and the buffy coat was performed according to manufacturer protocol using the Qiagen DNeasy Blood & Tissue Kit (Qiagen, CA, USA) and the Zymo Genomic DNA Clean & Concentrator Kit (Zymo Research, CA, USA). DNA sodium bisulfite conversion was conducted according to manufacturer protocol using the EZ-96 DNA Methylation-Direct and EZ DNA Methylation-Direct kits (Zymo Research). Blood and adipose tissue samples were distributed randomly across plates prior to analysis using the Infinium HumanMethylation450 BeadChip array (Illumina, CA, USA) at the UCSF Institute for Human Genetics, Genomics Core Facility (CA, USA), following standard Illumina protocols. Preprocessing of the methylation data was conducted as described in Huang *et al.* (2016) [19]. Briefly, background and dye-bias corrections were applied using the 'methylumi' package in R, normalization was performed using the β-Mixture Quantile Dilation approach and adjustments for batch effects

were made using linear mixed models [20]. After quality control and probe filtering, 285,163 CpG sites were included in the analyses.

Statistical analyses

Epigenome-wide two-stage mediation analyses

We conducted sex-specific two-stage epigenome-wide association scans (EWAS) for significance testing of putative CpG candidates by which methylation might mediate the effect of ELSD on adult BMI [21]. In the first stage, we conducted EWAS analyses to detect association between CpG methylation and adult BMI using the following model:

$$E\left(Y_i\right) = \beta_X^T X_i + \beta_S S_i + \beta_M M_i + \beta_{SM} S_i M_i \qquad \text{(Equation 1)}$$

where *Y, S, M* and *X* are adult BMI, ELSD, methylation M-value and the confounding covariates (including age, race, BMI at age 7, maternal smoking), for subject *i* respectively. Only those loci demonstrating sufficient evidence of association with BMI under a likelihood ratio test comparing [1] against a reduced model excluding all CpG effects and interaction terms were considered putative mediators. To screen the first-stage results, we applied a p-value threshold to identify significant CpG loci at $p < 0.005$.

For the second stage, we conducted EWAS analyses to detect the association between CpG methylation and ELSD among the CpG-BMI loci that met our first-stage criteria using the following model:

$$E\left(M_i\right) = \alpha_X^T X_i + \alpha_S S_i \qquad \text{(Equation 2)}$$

where *M, X* and *S* are defined as in [1]. Only those candidate CpG loci, which met the first-stage p-value threshold, and also demonstrated association with ELSD in the second stage, again at $p < 0.005$, were reported.

The above two-stage mediation analyses were conducted for DNAm in blood and adipose tissue separately. To adjust for potential confounding arising from cellular heterogeneity in blood tissue, cell mixture deconvolution (CMD) was performed using the method developed by Houseman *et al.* [22], and admixture estimates were included as adjustment covariates in the blood EWAS. CMD was not conducted in adipose tissue due to the lack of reference libraries for adipose tissue-specific differentially methylated regions and an insufficient sample size for a reference-free CMD approach.

Joint mediation analysis

The two-stage joint testing approach has been shown to be more powerful in identifying mediation effects via hypothesis testing [21], but it fails to provide estimates for the mediated effect of ELSD on adulthood BMI. We therefore implemented cross-product-based mediation analyses to quantify and test the direct effect (DE) and the indirect effect (IE) for the set of CpG loci that survived both levels of the two-stage approach [23–26]. Under the framework of causal inference, using potential outcomes and counterfactuals, the point estimates of the indirect (i.e., the mediation effect) and direct effects can be expressed by a combination of regression parameters of the above two models: $IE = \left(\beta_M \alpha_S + \beta_{SM} \alpha_S S_0\right)\left(S_1 - S_0\right)$ and $DE = \left(\beta_S + \beta_{SM}\left(\alpha_X^T X + \alpha_S S_0\right)\right)\left(S_1 - S_0\right)$, where S_0 and S_1 represent two different counterfactual realizations of ELSD. The corresponding variance and CIs were obtained via a bootstrap procedure. p-values were also calculated using the joint significance test (JST) as the maximum of the two stage p-values for each site [27]. For loci with DE and IE estimates in the same direction, proportion of mediation was calculated as IE/(IE + DE) to characterize the proportion of the total effect of ELSD on BMI mediated by methylation per site.

Pathway analysis

To investigate the enrichment of signals within genes belonging to common biological pathways, processes or gene sets, a broad base of genes inclusive of those with weaker signals is needed. In order to conduct pathway analyses, all CpG sites surviving a relaxed p-value threshold of $p < 0.01$ in the both stages of the two-stage mediation analyses were included for males and females. Because methylation data are comprised of specific sites, not all of which map to genes, a pathway approach which focuses on regulatory regions, rather than specific gene constructs, was implemented using the Genomic Regions Enrichment of Annotations Tool (GREAT) version 3.0 software

Table 1. Clinical and demographic characteristics of the Longitudinal Effects on Aging Perinatal sample.

Characteristics	Total (n = 143)	Males (n = 69)	Females (n = 74)
Age in years:			
– Mean (SD)	46.9 (1.7)	47.1 (1.6)	46.8 (1.8)
Race % (no.):			
– White	66.4 (95)	63.8 (44)	68.9 (51)
– Non white	33.6 (48)	36.2 (25)	31.1 (23)
Age 7 BMI:			
– Mean (SD)	16.3 (2.5)	16.5 (2.8)	16.1 (2.1)
Maternal cigarettes/day:			
– Median (IQR)	5 (0–20)	4.5 (0–20)	6 (0–20)
– Range	0–50	0–40	0–50
ELSD:			
– Median (IQR)	2.5 (1.5–4.0)	2.5 (1.375–4.0)	2.5 (1.5–4.0)
– Range	0–8	0–8	0–6.5
Adult BMI:			
– Mean (SD)	31.5 (7.4)	31.7 (5.8)	31.3 (8.7)
– Range	19.4–65.5	21.2–46.1	19.4–65.5

BMI: Body mass index; ELSD: Early life social disadvantage (age 7); IQR: Interquartile range; SD: Standard deviation.

(Bejerano Lab, CA, USA) using default parameters [28]. Input regions for each CpG site were specified as ±2 bp on either side of the genomic location of the CpG. Enrichment terms significant at $p < 0.005$ by both the binomial and hypergeometric enrichment tests and with binomial fold enrichment greater than two were obtained, and those with false discovery rate $Q < 0.1$ were reported. As before, males and females were analyzed separately.

Results

Clinical & demographic characteristics of the sample

The mean age at assessment in the final analytic sample (n = 143) was 46.9 years, and study subjects were mostly white (66.4%) and female (51.8%). Distributions of the different characteristics across both males and females were consistent with distributions in the full LEAP sample (n = 400). The clinical and demographic features of the sample are summarized in Table 1.

ELSD-BMI candidate-mediating loci are sex & tissue specific

In the two-stage EWAS analyses, adipose tissue methylation at 32,100 and 5757 out of 285,163 CpG sites were identified as associated with BMI after surviving the first-stage p-value threshold in males and females, respectively. Of the surviving first-stage CpG loci, 28 sites in males and 131 sites in females were identified as jointly significant with ELSD on BMI at $p < 0.005$ (Supplementary Tables 1 & 2) in the second stage. Mediating methylation loci were unique in females and males; no candidate-mediating sites common to both sexes were present. Cross-product-based mediation analyses revealed 22 candidate CpG sites in males and 100 in females with evidence of mediating the effect of ELSD on adulthood BMI (p-value for indirect effect [$p_{indirect}$] < 0.05) (Tables 2, 3 & Supplementary Table 3), providing additional support for the intermediary role played by these loci. In the two-stage analysis of peripheral blood leukocytes, 1882 and 895 loci survived the first stage in males and females, respectively. No loci survived second-stage thresholding in males. Three loci survived in females but none were identified as significant mediators in cross-product-based analyses (Supplementary Table 3). Thus, no candidate-mediating loci were further investigated in peripheral blood leukocytes.

The CpG sites with the strongest evidence for mediation in female adipose tissue (i.e., those with the most significant cross-product-based indirect effects) were: cg04145890 ($p_{indirect} < 0.001$, p-value for joint significance test [p_{JST}] = 1.62×10^{-4}) in *FGFRL1*, cg26750548 ($p_{indirect} < 0.001$, $p_{JST} = 0.001$) *LDB3*, and cg1195015 ($p_{indirect} < 0.001$, $p_{JST} = 0.002$) in *FASN*. Several genes included multiple top hits. The multihit genes included: *ADAM5P* with cg11199639 ($p_{indirect} = 0.014$, $p_{JST} = 0.002$), cg19659741 ($p_{indirect} = 0.02$, $p_{JST} = 0.003$), cg07387286 ($p_{indirect} = 0.066$, $p_{JST} = 0.004$); *BCAR3* with cg17274827 ($p_{indirect} = 0.002$, $p_{JST} = 0.003$) and cg15925478 ($p_{indirect} = 0.05$, $p_{JST} = 0.002$); *PHKG1* with cg26422861 ($p_{indirect} = 0.01$, $p_{JST} = 0.002$) and

Table 2. Mediation effects for top 22 loci in male adipose tissue surviving the two-stage mediation analysis thresholds and with indirect p-value <0.05.

CpG ID	Chr	Gen Loc	Gene	Gene group	Re: CGI	p(S->Mj)	p(Mj->BMI)	Indirect	95% CI	$p_{indirect}$	Direct	95% CI	p_{direct}	R^2	Prop.Med
cg08996506	16	16070868	ABCC1	Body		1.22E-04	0.001‡	0.922	(0.397–1.5)	<0.001	0.196	(-0.853–1.28)	0.808	0.054	0.825
cg23644736	1	55544866	USP24	Body		0.003‡	1.13E-04	0.817	(0.319–1.38)	<0.001	0.253	(-0.645–1.48)	0.678	0.208	0.764
cg15230985	17	78753887	RPTOR	Body		0.004‡	2.34E-06	0.997	(0.436–1.68)	0.002	0.478	(-0.507–1.69)	0.402	0.159	0.676
cg18573842	6	30139421	TRIM15	Body	N_Shore	0.001	0.001‡	-0.662	(-1.26 to -0.229)	0.002	0.691	(-0.234–1.79)	0.148	0.123	
cg26106417	4	3425381	RGS12	Body		0.002	0.004‡	0.790	(0.261–1.42)	0.002	0.159	(-0.847–1.28)	0.896	0.108	0.832
cg26390400	5	10556455				0.002	0.002‡	0.850	(0.323–1.42)	0.002	0.391	(-0.568–1.27)	0.470	0.099	0.685
cg03657040	5	175083981	HRH2	TSS1500	N_Shore	0.003‡	0.001	0.745	(0.198–1.51)	0.004	0.064	(-0.908–1.18)	0.982	0.108	0.921
cg10893483	1	156712783	HDGF	3′UTR	S_Shore	0.003	0.005‡	0.675	(0.142–1.77)	0.004	0.398	(-0.464–1.59)	0.428	0.066	0.629
cg23588713	12	56523270	ESYT1	Body	Island	0.003‡	0.001	0.603	(0.175–1.15)	0.004	-0.495	(-1.48–0.308)	0.152	0.131	
cg25277723	6	137072948	MAP3K5	Body		0.001‡	4.86E-04	-0.744	(-1.48 to -0.16)	0.004	0.422	(-0.643–1.37)	0.394	0.117	
cg06852605	17	76422640	DNAH17	Body	S_Shore	0.004‡	0.001	0.752	(0.179–1.49)	0.006	0.16	(-0.651–1.06)	0.816	0.126	0.825
cg08062812	1	91191232			Island	0.001‡	0.001	-0.769	(-1.65 to -0.223)	0.006	0.329	(-0.659–1.82)	0.496	0.103	
cg17334453	17	14479244				0.004‡	1.29E-04	0.799	(0.312–1.400)	0.006	-0.172	(-0.896–0.678)	0.628	0.096	
cg24162251	14	32420205				0.003‡	0.002	-0.618	(-1.100 to -0.143)	0.006	0.308	(-0.502–1.290)	0.426	0.140	
cg14319235	1	79472282	ELTD1	Body	Island	0.004	0.005‡	-0.591	(-1.340 to -0.113)	0.008	0.217	(-0.799–1.170)	0.660	0.087	
cg15056348	10	134350107	INPP5A	TSS1500	N_Shore	3.13E-04‡	6.17E-05	-0.949	(-1.880 to -0.309)	0.010	0.508	(-0.538–1.800)	0.334	0.213	
cg09730801	17	48048875	DLX4	Body; TSS1500	N_Shore	0.003‡	0.003	-0.574	(-1.270 to -0.094)	0.014	0.414	(-0.693–1.500)	0.462	0.151	
cg10793301	20	56064194	HMGB1L1	TSS200		0.005‡	0.003	0.606	(0.121–1.380)	0.016	0.256	(-0.737–1.210)	0.686	0.067	0.703
cg25100475	1	227750970	ZNF678	TSS1500	N_Shore	0.004‡	0.002	0.679	(0.098–1.670)	0.018	0.586	(-0.347–1.540)	0.270	0.067	0.537
cg01021682	3	101926162				0.002‡	0.002	0.644	(0.084–1.300)	0.022	-0.235	(-1.170–0.654)	0.546	0.074	
cg01956154	14	94423399	ASB2	5′UTR; 1stExon		0.004	0.005‡	-0.523	(-1.110 to -0.058)	0.024	0.381	(-0.617–1.340)	0.392	0.131	
cg24243753†	6	97972900				0.005‡	2.59E-04	-0.553	(-1.410 to -0.018)	0.044	0.603	(-0.334–1.720)	0.204	0.170	

† Denotes sites that were also identified as mediating candidates in prior mediation analyses for socioeconomic status and BMI in the same cohort.

‡ Denotes the joint significance test p-values, i.e., the maximum p-value from each stage of the two-stage mediation testing analyses.

Chr: Chromosome number; Direct: Direct effect; FDR(Mj->BMI): False discovery rate for association of methylation mediator with BMI; Gen Loc: Genetic location; Indirect: Indirect effect of methylation mediator in association of early life social disadvantage with BMI; p_{direct}: p-value for direct effect; $p_{indirect}$: p-value for indirect effect; p(Mj->BMI): p-value for association of methylation mediator with BMI; p(S->Mj): p-value for association of early life social disadvantage with methylation mediator; Prop.Med: Proportion of total association between early life social disadvantage and BMI explained by DNA methylation (calculated indirect effect/[indirect effect + direct effect]; applicable only if indirect and direct effects are in the same direction); R^2: Marginal coefficient of variation; Re: CGI: Relationship to canonical CpG island; S: Early life social disadvantage at age 7 years.

Table 3. Mediation effects for 27 selected top loci in female adipose tissue surviving the two-stage mediation analysis thresholds and with indirect p-value < 0.05.

CpG ID	Chr	Gen Loc	Gene	Gene group	Re: CGI	p(S->Mj)	p(Mj->BMI)	Indirect	95% CI	$p_{indirect}$	Direct	95% CI	p_{direct}	R^2	Prop.Med
cg04145890	4	1007657	FGFRL1	Body	S_Shore	1.62E-04‡	2.07E-05	1.350	(0.557–2.320)	<0.001	1.150	(-0.096–2.300)	0.068	0.366	0.540
cg26750548†	10	88441152	LDB3	Body		0.001	0.001‡	0.930	(0.281–1.920)	<0.001	1.150	(-0.063–2.260)	0.056	0.322	0.447
cg11950105†	17	80050646	FASN	Body	Island	0.002‡	0.001	0.682	(0.248–1.350)	<0.001	0.790	(-0.269–1.970)	0.134	0.308	0.463
cg21103829	5	140054320	DND1; HARS	TSS1500; Body	S_Shore	0.001	0.002‡	1.160	(0.385–2.240)	<0.001	1.340	(0.012–2.660)	0.048	0.298	0.464
cg17977470	17	7758854	TMEM88	Body	Island	0.004‡	0.001	0.729	(0.262–1.400)	0.002	1.160	(0.034–2.280)	0.046	0.301	0.386
cg18410680†	17	7758397	TMEM88	1stExon	N_Shore	0.002	0.005‡	0.878	(0.143–1.840)	0.022	1.260	(0.174–2.370)	0.024	0.345	0.411
cg16641055	16	88846292	PIEZO1§	Body	S_Shore	0.002	0.003‡	0.851	(0.275–1.650)	0.002	1.300	(-0.037–2.540)	0.066	0.277	0.396
cg27630153†	16	88845038	PIEZO1§	Body	Island	0.001	0.003‡	0.598	(0.066–1.390)	0.018	0.747	(-0.419–1.910)	0.184	0.304	0.445
cg17274827†	1	94075555	BCAR3	Body		0.001	0.003‡	1.070	(0.316–2.030)	0.002	1.910	(0.796–2.960)	0.002	0.167	0.359
cg15925478	1	94081080	BCAR3	Body		0.002‡	3.55E-04	0.600	(0.006–1.350)	0.050	0.766	(-0.133–1.740)	0.110	0.370	0.439
cg02655351	1	3498101	MEGF6	Body	N_Shore	0.001‡	1.96E-04	0.825	(0.249–1.750)	0.004	0.771	(-0.354–1.820)	0.158	0.384	0.517
cg01993576	6	44187674	SLC29A1	5′UTR	S_Shore	0.001	0.003‡	0.764	(0.214–1.490)	0.004	1.030	(-0.373–2.210)	0.134	0.271	0.426
cg07568841	7	30362781	ZNRF2	Body		3.55E-05	0.005‡	0.986	(0.302–1.890)	0.004	1.010	(-0.729–2.410)	0.254	0.334	0.494
cg12793803	17	62084217	ICAM2	5′UTR;1stExon		0.003‡	8.82E-04	0.652	(0.188–1.270)	0.004	0.911	(-0.128–1.930)	0.088	0.334	0.417
cg26422861	7	56160737	PHKG1	TSS200		0.002‡	3.68E-04	1.150	(0.254–2.200)	0.010	1.210	(0.012–2.200)	0.050	0.388	0.487
cg08370546	7	56160770	PHKG1	TSS200		0.002‡	0.002‡	0.811	(0.042–1.790)	0.042	1.070	(-0.071–2.180)	0.074	0.385	0.431
cg10780949	15	67418316	SMAD3	Body; 1stExon; 5′UTR		0.002‡	0.002	0.730	(0.155–1.570)	0.012	1.010	(-0.283–2.060)	0.138	0.316	0.420
cg11199639	8	39172111	ADAM5P	TSS200		0.001	0.002‡	0.975	(0.183–1.940)	0.014	1.200	(0.254–2.310)	0.020	0.344	0.448
cg19659741	8	39172099	ADAM5P	TSS200		0.002	0.003‡	0.567	(0.040–1.480)	0.020	0.941	(0.008–2.080)	0.046	0.341	0.376
cg07387286	8	39172120	ADAM5P	TSS200		0.003	0.004‡	0.699	(-0.024–1.860)	0.066	1.100	(0.042–2.310)	0.038	0.330	0.389
cg11981599	8	11566526	GATA4	Body	Island	2.20E-04	2.49E-04‡	0.888	(0.144–1.820)	0.016	0.674	(-0.505–1.880)	0.226	0.365	0.569
cg25840926†	2	20647987	RHOB	1stExon; 3′UTR	Island	3.86E-05	0.005‡	0.984	(0.155–1.760)	0.018	1.010	(-0.135–2.060)	0.092	0.329	0.493
cg25490145†	17	80358850	C17orf101	Body	N_Shelf	3.40E-05	0.001‡	0.789	(0.144–1.550)	0.020	0.413	(-0.895–1.540)	0.512	0.399	0.656
cg02422603†	13	114890566	RASA3	Body		0.001	0.003‡	0.900	(0.155–1.820)	0.022	1.110	(-0.192–2.490)	0.084	0.303	0.448
cg02907425	19	4688820	DPP9	Body	Island	0.003	0.005‡	0.874	(0.067–2.040)	0.034	1.390	(0.288–2.430)	0.016	0.380	0.386
cg16582779	14	29237202	FOXG1	1stExon	Island	0.001	0.003‡	0.535	(0.040–1.330)	0.036	0.725	(-0.536–1.870)	0.230	0.389	0.425
cg16145324	6	36020012	MAPK14	Body		0.002‡	6.38E-04	0.809	(0.270–1.580)	0.002	1.060	(-0.025–1.990)	0.052	0.367	0.433

†Denote sites that were also identified as mediating candidates in prior mediation analyses for socioeconomic status and BMI in the same cohort.

‡Italicized p-values denote the joint significance test p-values, i.e., the maximum p-value from each stage of the two-stage mediation testing analyses.

§PIEZO1 was previously known as FAM38A.

Chr: Chromosome number; Direct: Direct effect; FDR(Mj->BMI): False discovery rate for association of methylation mediator with BMI; Gen Loc: Genetic Location; Indirect: Indirect effect of methylation mediator in association of early life social disadvantage with BMI; p_{direct}: p-value for direct effect; $p_{indirect}$: p-value for indirect effect; p(Mj->BMI): p-value for association of methylation mediator with BMI; p(S->Mj): p-value for association of early life social disadvantage with methylation mediator; Prop.Med: Proportion of total association between early life social disadvantage and BMI explained by DNA methylation (calculated indirect effect/[indirect effect + direct effect]; applicable only if indirect and direct effects are in the same direction); R^2: Marginal coefficient of variation; Re: CGI: Relationship to canonical CpG island; S: Early life social disadvantage at age 7 years.

cg08370546 ($p_{indirect}$ = 0.042, p_{JST} = 0.002); *PIEZO1* with cg16641055 ($p_{indirect}$ = 0.002, p_{JST} = 0.003) and cg27630153 ($p_{indirect}$ = 0.018, p_{JST} = 0.003); and *TMEM88* with cg17977470 ($p_{indirect}$ = 0.002, p_{JST} = 0.004) and cg18410680 ($p_{indirect}$ = 0.022, p_{JST} = 0.005).

In males, notable CpG sites with the strongest evidence for mediation in adipose tissue were: cg08996506 ($p_{indirect} < 0.001$, p_{JST} = 6.44E-04) in *ABCC1*; cg23644736 ($p_{indirect} < 0.001$, p_{JST} = 0.003) in *USP24*; cg15230985 ($p_{indirect}$ = 0.002, p_{JST} = 0.004) in *RPTOR*; and cg25277723 ($p_{indirect}$ = 0.004, p_{JST} = 0.001) in *MAP3K5*.

ELSD, methylation, BMI & associated biological processes in adipose tissue

After relaxing the p-value thresholds in the two-stage analyses, a total of 109 and 397 CpG sites were selected for pathway analysis in male and female adipose tissue, respectively. GREAT analyses in males yielded only two nonspecific cancer-related enrichment terms (Supplementary Table 5). In females, the top pathway analysis results identified 32 enrichment terms (Table 4). These terms largely fell into categories associated with immunologic signatures of gene regulation in various leukocytes including macrophages, dendritic and T cells. Notable identified pathways with high fold-enrichment scores included MAPK and bone morphogenetic protein receptor signaling pathways.

Discussion

This study identified a number of novel CpG loci with statistical evidence of mediating the association between ELSD and adult adiposity as measured by BMI. These loci were tissue and sex specific; significant CpG sites were identified only in fat tissue and were unique between males and females. It is unclear why such a greater number of CpG loci were associated with BMI in stage one of our mediation analyses among males (77,245 CpGs) versus females (8868 CpGs). However, this may be in part due to sex specificity of epigenetic pathways contributing to adiposity: male adiposity might be influenced by a larger, more varied range of epigenetic pathways than female adiposity, which might be influenced by more specific mechanisms such as those affected by ELSD.

Notably, one of our top mediating sites in females was cg04145890, a CpG site mapping to *FGFRL1* which was also recently implicated in a Finnish monozygotic twin study of the association between methylation and BMI in adipose tissue [11], though at a different site. Interestingly, a large number of mediating loci identified in female fat tissue analyses localized to genes known to have associations with adipogenesis in obesity, insulin sensitivity and diabetes. For example, *DPP9* inhibition was shown to impair adipocyte differentiation by inhibiting PPARγ induction [29]. Increased expression of *FASN* has been linked to higher visceral fat accumulation and insulin resistance in humans [30], and obesogenic feeding in mice has been show to upregulate *FASN* expression and to associate with specific methylation signatures [31]. Among the multihit genes, *ADAM5P* belongs to the disintegrin and metalloproteinase family of genes, which are regulators of cellular adhesion, migration and signaling. ADAMs have been implicated in a number of human diseases, and play a role in both normal and pathogenic inflammatory responses (Figure 1) [32,33]. However, the specific literature for *ADAM5P* in adipogenic or inflammatory processes is limited. With respect to the other multisite genes: *BCAR3* has been implicated in genome wide association (GWA) loci interactions for diabetes [34] and is involved in the TGF-β signaling pathway, which plays a key role in both insulin resistance and adipogenesis [35,36]; and *PHKG1*, which is involved in the encoding of a catalytic subunit of phosphorylase kinase thus contributing to the cascade activation of glycogen breakdown, and in which mutations can cause a rare form of glycogen storage disease [37].

Top mediating sites in males did not include multihit genes; however, the analyses revealed several biologically plausible genes associated with inflammation and insulin resistance. In particular, these included *RPTOR*, which when disrupted in macrophages was shown to reduce inflammation and insulin resistance in mice experiments [38,39].

In the methylation profile of *PHKG1* (Figure 1), robust associations between ELSD and DNAm (blue line), and DNAm and BMI (green line), and significant indirect effect (red line) were observed in the CpG sites located within 200–1500 bp of the transcription start site, the 5′UTR or the first exon. In total, 7 of 14 methylation sites in *PHKG1* demonstrated significant mediation at $p < 0.05$. In *MAP3K5* (Figure 2), 2 of 21 methylation sites were significant for a mediation effect, and at each of these sites, a correspondingly robust signal was observed in the ELSD-DNAm and DNAm-BMI effects. Similar analyses for the other genes revealed: 3 of 25 sites in *FGFRL1*, 2 of 9 sites in *ADAM5P*, 2 of 14 sites in *BCAR3*, 1 of 16 sites in *DPP9*, 1 of 6 sites in *MAPK14*, and 2 of 286 sites in *RPTOR*.

The top sites presented in this study also included several loci which were consistent with sites identified in previous work exploring sex-specific adipose tissue epigenetic mediation between childhood SES and adulthood

Table 4. Female adipose tissue Genomic Regions Enrichment of Annotations Tool pathway analysis results.

GREAT v3.0.0 (hg19)		AR: Basal + extension: 5 Kb upstream, 1 Kb downstream, 1 Mb maximum extension, curated regulatory domains included										
Enrichment	Terms	Binomial test					Hypergeometric test					
		p-value	FDR Q	FE	Obs. R. hits	RSC	p-value	FDR Q	FE	Obs. G hits	Tot. genes	GSC
GO MF	RNA polymerase II transcription factor binding	3.25E-04	0.092	2.865	15	0.038	1.36E-06	0.002	4.721	14	88	0.023
MSigPW	Map kinase inactivation of SMRT corepressor	1.16E-04	0.031	8.133	6	0.015	3.49E-04	0.077	10.790	4	11	0.007
MSigPW	Genes involved in activated TAK1 mediates p38 MAPK activation	1.46E-04	0.028	7.789	6	0.015	1.29E-05	0.017	10.473	6	17	0.010
MSigPW	BMP receptor signaling	6.95E-04	0.057	3.519	10	0.025	6.81E-05	0.022	5.652	8	42	0.013
MSigPW	Genes involved in YAP1- and WWTR1 (TAZ)-stimulated gene expression	8.15E-04	0.060	4.745	7	0.018	1.14E-04	0.030	7.418	6	24	0.010
MSigPW	Genes involved in nucleotide-binding domain, leucine rich repeat containing receptor (NLR) signaling pathways	1.18E-03	0.078	4.448	7	0.018	1.91E-05	0.013	5.806	9	46	0.015
MSigPb	Genes upregulated in DO11.10 cells (hybridoma) by expression of transcriptionally activating form of HDAC7 [GeneID = 51564] and downregulated by its transcriptionally repressing form	1.47E-08	0.000	4.026	24	0.060	2.22E-05	0.011	2.983	19	189	0.031
MSigPb	Genes upregulated in luminal-like breast cancer cell lines compared with the mesenchymal-like ones	3.21E-06	0.005	2.443	33	0.083	3.85E-05	0.014	2.195	31	419	0.051
MSigPb	Genes downregulated in polysomal and total RNA samples from SW480 cells (primary colorectal carcinoma) compared with the SW620 cells (lymph node metastasis from the same individual)	5.60E-06	0.006	3.389	19	0.048	3.32E-06	0.006	3.709	17	136	0.028
MSigPb	Upregulated genes in B-cell chronic lymphocytic leukemia patients expressing high levels of ZAP70 and CD38 [GeneID = 7535;952], which are associated with poor survival	6.74E-06	0.006	2.638	27	0.068	9.31E-05	0.026	2.473	22	264	0.036
MSigPb	Transcripts depleted from pseudopodia of NIH/3T3 cells (fibroblast) in response to haptotactic migratory stimulus by fibronectin, FN1 [GeneID = 2335]	9.47E-06	0.006	2.063	42	0.106	9.11E-04	0.093	1.714	38	658	0.063
MSigPb	Extracellular matrix (ECM) related genes upregulated early (within 30 min) in dermal fibroblasts after addition of TGFB1 [GeneID = 7040]	1.69E-05	0.007	4.606	12	0.030	2.18E-04	0.043	4.307	9	62	0.015
MSigPb	Genes downregulated in liver tumor compared with the normal adjacent tissue	1.80E-05	0.006	2.742	23	0.058	6.57E-04	0.082	2.248	20	264	0.033
MSigPb	Genes upregulated in T98 cells (glioma) 48 h after treatment with IFN-β	5.51E-05	0.015	3.795	13	0.033	6.78E-04	0.081	3.709	9	72	0.015
MSigPb	Genes that cooperate with MYC and TBX2 [GeneID = 4609;6909] to transform MEF cells (mouse embryonic fibroblasts)	1.34E-04	0.028	15.912	4	0.010	5.09E-04	0.075	9.891	4	12	0.007
MSigPb	Genes downregulated in freshly isolated CD31- [GeneID = 5175] (stromal stem cells from adipose tissue) versus the $CD31^+$ (nonstem) counterparts	1.54E-04	0.029	2.321	24	0.060	3.68E-05	0.015	2.786	20	213	0.033
MSigPb	Cluster P7 of genes with similar expression profiles in peripheral T lymphocytes after FOXP3 [GeneID = 50943] loss of function	2.32E-04	0.034	3.102	14	0.035	1.29E-04	0.029	3.840	11	85	0.018
MSigPb	Cluster 2: ECM-related genes upregulated in dermal fibroblasts within 30 min after TGFB1 [GeneID = 7040] addition; reached a plateau after that	2.54E-04	0.030	5.789	7	0.018	2.86E-04	0.051	6.358	6	28	0.010

FDR Q: False discovery rate Q statistic; FE: Fold enrichment; G: Genes; GO MF: Gene ontology molecular function; GSC: Gene set coverage; MSigIS: MSigDB immunologic signature; MSigOS: MSigDB oncogenic signature; MSigPB: MSigDB perturbation; MSigPW: MSigDB pathway; Obs.: Observed; R: Region; RSC: Region set coverage; Tot.: Total.

Table 4. Female adipose tissue Genomic Regions Enrichment of Annotations Tool pathway analysis results (cont.).

GREAT v3.0.0 (hg19)		AR: Basal + extension: 5 Kb upstream, 1 Kb downstream, 1 Mb maximum extension, curated regulatory domains included										
Enrichment	Terms	Binomial test					Hypergeometric test					
		p-value	FDR Q	FE	Obs. R. hits	RSC	p-value	FDR Q	FE	Obs. G hits	Tot. genes	GSC
MSigPb	Downregulated genes in both rectal and colon carcinoma compared with normal mucosa samples	5.87E-04	0.055	2.963	13	0.033	3.83E-04	0.061	3.400	11	96	0.018
MSigOS	Genes upregulated in a panel of epithelial cell lines by TGFB1 [Gene ID = 7040]	6.19E-06	0.001	2.650	27	0.068	1.43E-08	0.000	3.870	24	184	0.039
MSigIS	Genes upregulated in comparison of dendritic cells stimulated with R848 at 2 h vs DCs stimulated with R848 for 8 h	4.83E-07	0.001	3.688	21	0.053	1.80E-04	0.049	2.727	17	185	0.028
MSigIS	Genes upregulated in comparison of monocytes cultured for 0 days vs those cultured for 1 day	1.28E-06	0.001	3.234	23	0.058	3.78E-04	0.056	2.561	17	197	0.028
MSigIS	Genes upregulated in comparison of macrophages exposed to 5 worms/well *Brugia malayi* vs macrophages exposed to *Mycobacterium tuberculosis*	6.40E-06	0.003	3.019	22	0.055	1.11E-04	0.053	2.739	18	195	0.030
MSigIS	Genes downregulated in comparison of macrophages treated with IL25 [GeneID = 64806] versus neutrophils treated with IL25 [GeneID = 64806]	6.95E-06	0.003	2.833	24	0.060	8.86E-07	0.002	3.314	22	197	0.036
MSigIS	Genes downregulated in comparison of dendritic cells stimulated with Pam3Csk4 (TLR1/2 agonist) at 12 h vs dendritic cells stimulated with Gardiquimod (TLR7 agonist) at 12 h	7.50E-06	0.002	2.988	22	0.055	2.59E-06	0.002	3.212	21	194	0.035
MSigIS	Genes upregulated in comparison of macrophages exposed to *Toxoplasma gondii* vs macrophages exposed to *M. tuberculosis*	2.10E-05	0.004	2.971	20	0.050	5.98E-04	0.076	2.461	17	205	0.028
MSigIS	Genes downregulated in comparison of dendritic cells exposed to *T. gondii* vs macrophages exposed to *T. gondii*	4.52E-05	0.008	2.649	22	0.055	1.11E-04	0.053	2.739	18	195	0.030
MSigIS	Genes upregulated in comparison of type 2 myeloid (T2M) cells treated with IL25 [GeneID = 64806] vs neutrophils treated with IL25 [GeneID = 64806]	9.63E-05	0.014	2.656	20	0.050	3.36E-04	0.058	2.587	17	195	0.028
MSigIS	Genes upregulated in comparison of dendritic cells stimulated with poly(I:C) (TLR3 agonist) at 24 h vs dendritic cells stimulated with Pam3Csk4 (TLR1/2 agonist) at 24 h	9.96E-05	0.014	2.649	20	0.050	1.11E-04	0.053	2.739	18	195	0.030
MSigIS	Genes upregulated in comparison of untreated CD4 [GeneID = 920] T cells at 0 h vs the untreated cells at 4 h	1.22E-04	0.015	2.690	19	0.048	3.32E-04	0.063	2.682	16	177	0.026
MSigIS	Genes upregulated in comparison of peripheral blood mononuclear cells from healthy donors vs peripheral blood mononuclear cells from infants with acute RSV infection	1.66E-04	0.019	2.811	17	0.043	3.77E-04	0.060	2.652	16	179	0.026
MSigIS	Genes upregulated in comparison of dendritic cells stimulated with lipopolysaccharide (LPS) (TLR4 agonist) at 16 h vs dendritic cells stimulated with Pam3Csk4 (TLR1/2 agonist) at 16 h	3.00E-04	0.027	2.668	17	0.043	3.16E-04	0.067	2.600	17	194	0.028

FDR Q: False discovery rate Q statistic; FE: Fold enrichment; G: Genes; GO MF: Gene ontology molecular function; GSC: Gene set coverage; MSigIS: MSigDB immunologic signature; MSigOS: MSigDB oncogenic signature; MSigPB: MSigDB perturbation; MSigPW: MSigDB pathway; Obs.: Observed; R: Region; RSC: Region set coverage; Tot.: Total.

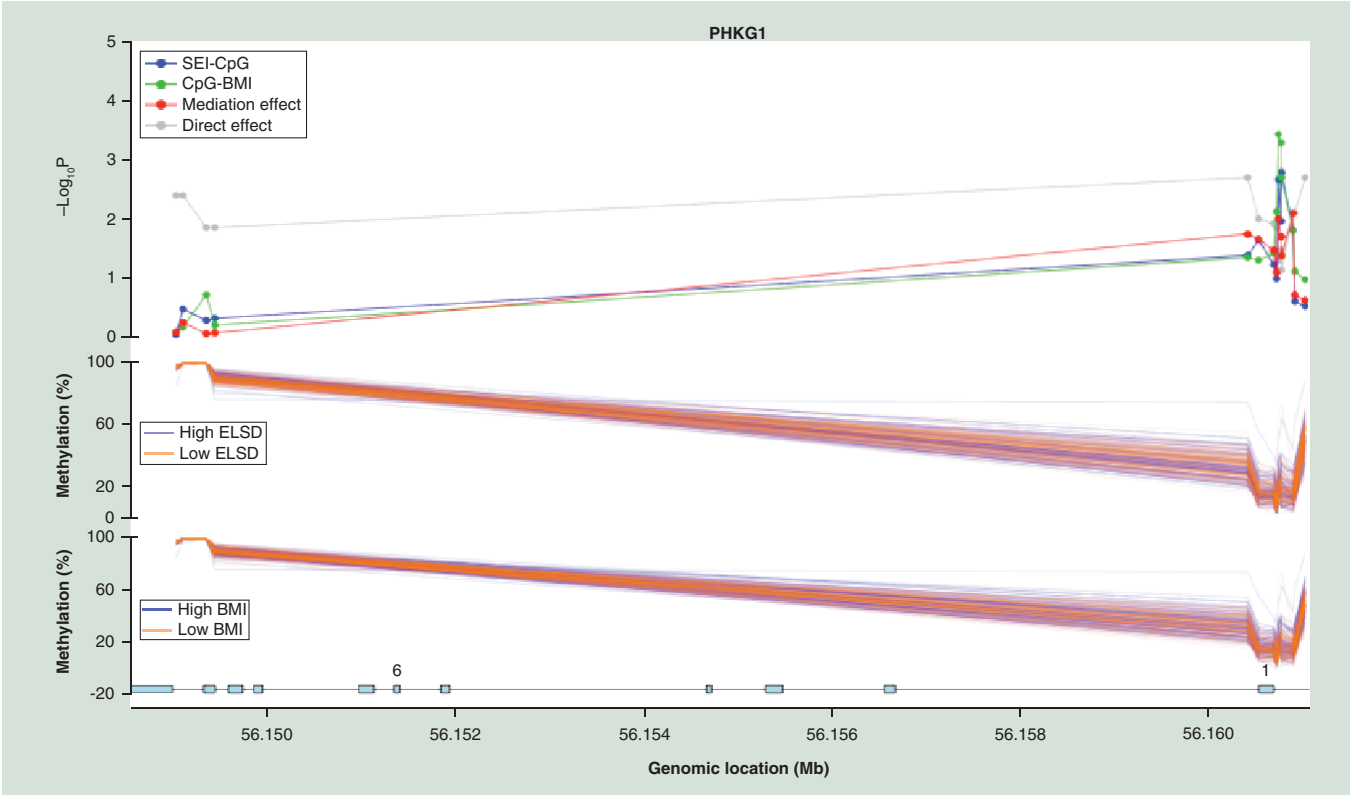

Figure 1. Mediation analysis of methylation profiles across *PHKG1* CpG sites in female adipose tissue.

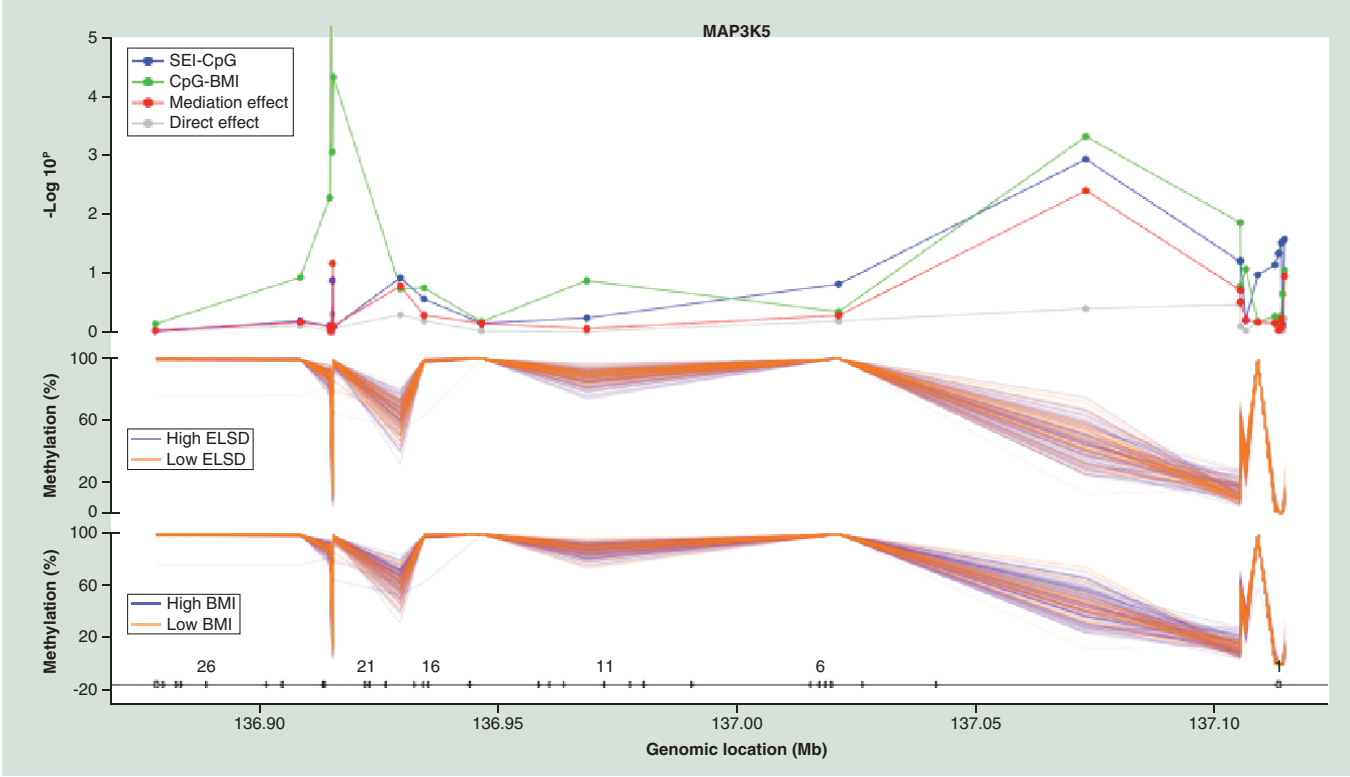

Figure 2. Mediation analysis of methylation profiles across *MAP3K5* CpG sites in male adipose tissue.

adiposity in the same cohort [40]. Specifically, among our top findings, 1 CpG site in men and 11 CpG sites in women were also observed in the top hits from the childhood SES analyses (Tables 2 & 3). As our measure of ELSD was inclusive of measures of childhood SES, while encompassing additional measures of environmental and psychosocial adversity (e.g., changes in parent's marital status, death of a sibling), overlapping findings were not unexpected. Indeed, the fact that some methylation sites were common to different, but related, early life constructs lend further credibility to the results presented here. Sensitivity analyses adjusting for childhood socioeconomic index in the association between ELSD, DNAm and BMI, can be viewed in Supplementary Table 6.

MAPK signaling in adipose tissue

Unique MAPK-related signals were discovered in both male and female adipose mediation analyses, and MAPKs were also involved in significant enrichment terms in the female pathway analyses. Specifically, *MAP3K5* and *MAPK14* were identified as potential sites of ELSD-BMI mediation in males and females, respectively. In a recent study, *MAP3K5* mRNA and protein expression was shown to be upregulated in adipose tissue by transcription factor *E2F1* vis-à-vis JNK-mediated sensitization to activation at the *MAP3K5* promoter [41].*MAPK14* modulates glucose metabolism and limits autophagy in nutrient-deprived conditions [42]. Genetic variants in *MAPK14* were recently associated with diabetic foot ulcers [43], and a low-frequency variant in *MAPK14* was also found to associate with myeloperoxidase, a biomarker for cardiovascular events [44]. More generally, *MAPK* signaling pathways and their constituents have been found to associate with a number of stress-induced obesogenic processes in adipose tissue including: regulation of adipose tissue inflammation and insulin resistance [45], and adipogenesis [46].

Biological pathways from ELSD to obesity

A number of plausible pathways linking early life social environments and DNAm can be found in existing literature, including the classic findings of Weaver *et al.* [47] on the effect of early life maternal care on the epigenetic profiles of rat pups, and the reversibility of these differences through cross fostering to effect a stable change lasting into adulthood. This study and several that followed successfully established the notion of persistent epigenetic modifications induced by social programming [2,3,48,49]. In human studies, the more specific mechanisms by which the early life social environment might impact epigenetic patterns span hypotheses that posit the role of nutrition [50], modified stress responses [1,5–9,51] and altered immune system function [52,53]. Meanwhile, the connection between adiposity and altered methylation profiles has been extensively explored in blood tissue [54–59], and more recently several studies have also been conducted in the more biologically relevant adipose tissue [11,13,19,60]. The common thread connecting all of these studies is the likely role of epigenetic mechanisms as a mediator between early life social environments and health outcomes later in life.

Our findings in adipose tissue were sex specific. This is consistent with previous studies suggesting that epigenetic mechanisms and patterns differ by sex [13,15,61], including a recent study which identified within-pair differential DNAm patterns comparing monozygotic male and female pairs, suggesting differential sensitivity to methylation by sex [17]. The effects of socioeconomic gradients also have been shown to have stronger associations with adiposity in females than males [18]. We identified CpG loci in males and females that mapped to genes associated with adipogenesis, inflammation, diabetes and insulin resistance. That both male and female candidate mediation loci implicated adipogenesis, inflammatory and insulin signaling pathways, either via a gene hit or through pathway enrichment, is compelling – a rich body of literature has consistently connected ELSD, maladaptive stress responses and proneness to inflammation [53,62–70], all of which have well-established associations with adiposity. More specifically, the prevailing 'toxic stress' hypothesis suggests stress induced by a social environment can become 'toxic' by negatively modifying the epigenetic landscape in ways that increase disease risk and persist across time [71]. For example, social stressors in early life have been found to induce changes in the functioning of the hypothalamic–pituitary–adrenal axis, thereby reducing glucocorticoid and increasing proinflammatory signaling [9,53,72]. Such stress-related hormonal changes in the action of the hypothalamic–pituitary–adrenal axis could potentially modify epigenetic regulation of adipose tissue in a systemic manner, facilitating adipose dysregulation and contributing to obesity and cardiovascular risk. Indeed, very small changes in hormonal levels can have profound effects, and we cannot rule out either very small alterations that are not yet detectable with our current instruments or regulatory changes in CpGs associated with regulatory action that are not interrogated on the platform employed.

Strengths & limitations

This study sought to identify epigenetic mediators of ELSD on adult adiposity by using a rich source of existing data and biosamples from clinically relevant tissue sites: adipose tissue. Most existing studies of epigenetic alterations associated with ELSD and adiposity have been conducted in blood tissue, which has been shown to serve as precarious surrogate for adipose tissue [19]. Nonetheless, our findings must be interpreted with some caution as we were not able to adjust for potential cell admixture in the adipose tissue due to inadequate statistical power. Although methods for reference-free cell type adjustment exist [22], they require a large number of degrees of freedom that could not be accommodated with our sample size. Thus, it remains unclear whether the mediating CpG sites reported in this analysis were identified due to differential methylation patterns, or due to potential differences in adipose tissue composition between subjects with higher versus lower levels of ELSD. However, it is worth noting that there is an increasing body of literature that argues for assessing epigenetic effects in tissues that are relevant to the disease of interest. Adipose tissue is complex, and also includes blood in its composition. We reasoned that the blood cells in adipose tissue may exhibit completely different characteristics and concentrations in fat than in blood, and these features might themselves be important indicators of disease-associated processes.

The exposure-outcome data were obtained from a prospective, observational study, where methylation and BMI were measured simultaneously, leading to some limitations with respect to causal interpretations of our findings. Specifically, causal mediation analyses depend on certain assumptions regarding confounding: no unmeasured confounding between ELSD and methylation, methylation and BMI, and ELSD and BMI, and finally, no ELSD-induced confounder of the methylation and BMI relationship. Biologically, we are unable to distinguish with certainty the causal directionality of the BMI and methylation alterations with our current data. However, loss of methylation may arise either actively, via Tet enzyme-mediated action or through suppression of the DNA methyltransferase. The addition of methylation is likely DNA methyltransferase mediated, although the precise inducer of this action remains unknown. Since these biochemical dynamics take longer to evolve than the body weight changes, the assumption that BMI is affected by the DNAm may be more plausible than the reverse. Future exploration of these individual mechanisms is feasible and should be quite informative.

Although we followed conventional p-value thresholds, the selection of such cutoffs is generally arbitrary with limited theoretical justification in literature. Our two-stage p-value thresholds, however, were within range of similar studies [73–80]. The application of mediation analyses in a high-dimensional setting also increases the difficulty of multiple correction adjustment, which necessitates downstream review of the identified candidate sites for biological plausibility through, for example, support by prior literature or enrichment analysis.

Strengths of our analyses, beyond using appropriate tissue samples, include the prospective collection of ELSD measures during critical developmental periods in early childhood. We also used a composite measure of ELSD that encompassed parental socioeconomic indicators as well as childhood social environments and events, which directly captured multiple dimensions of the early life social experience. Additionally, the analytic methods included an efficient two-stage joint significance test for screening mediation effect in a genome-wide setting, an explicit estimation for the effect size of the mediation, and pathway analyses via GREAT. Standard approaches to pathway analysis are largely derived from gene expression data and are predicated on measuring the transcripts of biologically well-defined gene constructs. However, the analysis of methylation data, which typically amounts to specific sites, is likely better served by functional annotation analyses that focus on regulatory regions. By using GREAT, we were able to accommodate all candidate CpG sites regardless of whether they explicitly mapped to a gene, rather than discarding any nonmapped sites as in standard network analysis.

Conclusion

In summary, these results shed some light on potential epigenetic-mediating sites in adipose tissue which is likely the more relevant tissue for adiposity, and not peripheral blood leukocytes. Many of our mediation and pathway analyses results were consistent with findings in prior literature that have implicated inflammation and dysregulation of adipocytes in adipose tissue in obesogenic processes. Findings support the hypothesis that epigenetic pathways may play mediating roles in the associations of ELSD with adulthood adiposity.

Acknowledgements

The study protocol was approved by the institutional review boards at Brown University and Memorial Hospital of Rhode Island.

Summary points

- Early life social disadvantage with respect to socioeconomic position, structural social environments and psychosocial measures of adversity, was shown to associate with methylation patterns and increased risk for adulthood adiposity through unique biological mechanisms for men versus women.
- The effects of early life social disadvantage on adulthood adiposity were specific to adipose tissue; no mediation candidates were identified in peripheral blood.
- The majority of the mediating loci identified in female adipose tissue mapped to genes known to have associations with adipogenesis, diabetes, insulin sensitivity, PPARγ and TGF-β signaling pathways. Notable genes of interest included *FGFRL1*, *ADAM5P*, *BCAR3*, *DPP9* and *PIEZO1*.
- Functional gene groupings were less apparent in candidate mediation CpG sites in males than in females, but several loci in males mapped to genes associated with inflammation and signaling pathways: *RPTOR* and *MAP3K5*.
- Pathway analyses of mediation loci in female adipose tissue revealed compelling evidence of enrichment for immunologic signatures, and a number of MAPK-associated pathways.
- These findings are consistent with those in prior literature which have linked patterns of increased inflammation and adipocyte dysregulation in adipose tissue, and thereby also alterations in resident leukocyte populations, with increasing adiposity.

Financial & competing interests disclosure

This work was supported by the National Institute on Aging at the NIH (grant numbers RC2AG036666, R01AG048825), the Intramural Research Program of the Eunice Kennedy Shriver National Institute of Child Health and Human Development, and the Ministry of Science and Technology, Taiwan (grant number 105-2118-M-001-014-MY3). The authors have no other relevant affiliations or financial involvement with any organization or entity with a financial interest in or financial conflict with the subject matter or materials discussed in the manuscript apart from those disclosed.

No writing assistance was utilized in the production of this manuscript.

Ethical conduct of research

The authors state that they have obtained appropriate institutional review board approval or have followed the principles outlined in the Declaration of Helsinki for all human or animal experimental investigations. In addition, for investigations involving human subjects, informed consent has been obtained from the participants involved.

References

Papers of special note have been highlighted as: • of interest; •• of considerable interest

1. Gudsnuk K, Champagne FA. Epigenetic influence of stress and the social environment. *ILAR J.* 53(3–4), 279–288 (2012).
2. Szyf M, Weaver I, Meaney M. Maternal care, the epigenome and phenotypic differences in behavior. *Reprod. Toxicol.* 24(1), 9–19 (2007).
3. Szyf M. DNA methylation, behavior and early life adversity. *J. Genet. Genom.* 40(7), 331–338 (2013).
4. Tehranifar P, Wu H-C, Fan X *et al.* Early life socioeconomic factors and genomic DNA methylation in mid-life. *Epigenetics* 8(1), 23–27 (2013).
5. Needham BL, Smith JA, Zhao W *et al.* Life course socioeconomic status and DNA methylation in genes related to stress reactivity and inflammation: the multi-ethnic study of atherosclerosis. *Epigenetics* 10(10), 958–969 (2015).
6. Hoffmann A, Spengler D. The lasting legacy of social stress on the epigenome of the hypothalamic–pituitary–adrenal axis. *Epigenomics* 4(4), 431–444 (2012).
7. Tyrka AR, Price LH, Marsit C, Walters OC, Carpenter LL. Childhood adversity and epigenetic modulation of the leukocyte glucocorticoid receptor: preliminary findings in healthy adults. *PLoS ONE* 7(1), e30148 (2012).
8. Anacker C, O'Donnell KJ, Meaney MJ. Early life adversity and the epigenetic programming of hypothalamic–pituitary–adrenal function. *Dialogues Clin. Neurosci.* 16(3), 321–333 (2014).
9. Turecki G, Meaney MJ. Effects of the social environment and stress on glucocorticoid receptor gene methylation: a systematic review. *Biol. Psychiatry* 79(2), 87–96 (2016).
10. Martinez JA, Milagro FI, Claycombe KJ, Schalinske KL. Epigenetics in adipose tissue, obesity, weight loss, and diabetes. *Adv. Nutr.* 5(1), 71–81 (2014).
11. Pietiläinen KH, Ismail K, Järvinen E *et al.* DNA methylation and gene expression patterns in adipose tissue differ significantly within young adult monozygotic BMI-discordant twin pairs. *Int. J. Obes.* 40(4), 654–661 (2016).
12. Huang R-C, Galati JC, Burrows S *et al.* DNA methylation of the IGF2/H19 imprinting control region and adiposity distribution in young adults. *Clin. Epigenet.* 4(1), 21 (2012).

13. Agha G, Houseman EA, Kelsey KT, Eaton CB, Buka SL, Loucks EB. Adiposity is associated with DNA methylation profile in adipose tissue. *Int. J. Epidemiol.* 44(4), 1277–1287 (2015).
14. Dick KJ, Nelson CP, Tsaprouni L *et al.* DNA methylation and body-mass index: a genome-wide analysis. *Lancet* 383(9933), 1990–1998 (2014).
15. Appleton AA, Armstrong DA, Lesseur C *et al.* Patterning in placental 11-B hydroxysteroid dehydrogenase methylation according to prenatal socioeconomic adversity. *PLoS ONE* 8(9), e74691 (2013).
16. Zhang Z, Liu J, Kaur M, Krantz ID. Characterization of DNA methylation and its association with other biological systems in lymphoblastoid cell lines. *Genomics* 99(4), 209–219 (2012).
17. Watanabe M *et al.*, Osaka Twin Research Group, Yorifuji S *et al.* Within-pair differences of DNA methylation levels between monozygotic twins are different between male and female pairs. *BMC Med. Genomics* 9(1), 55 (2016).

• **Provides evidence of sex differences in DNA methylations in monozygotic twins, suggesting that methylation variability is higher in males than females across 80% of autosomal CpG islands.**

18. Senese LC, Almeida ND, Fath AK, Smith BT, Loucks EB. Associations between childhood socioeconomic position and adulthood obesity. *Epidemiol. Rev.* 31(1), 21–51 (2009).
19. Huang Y-T, Chu S, Loucks EB *et al.* Epigenome-wide profiling of DNA methylation in paired samples of adipose tissue and blood. *Epigenetics* 11(3), 227–236 (2016).

•• **Explores the nonexchangeability of adipose and blood tissue with respect to differential global and local methylation profiles by tissue type.**

20. Teschendorff AE, Marabita F, Lechner M *et al.* A β-mixture quantile normalization method for correcting probe design bias in Illumina Infinium 450 k DNA methylation data. *Bioinformatics* 29(2), 189–196 (2013).
21. MacKinnon DP, Lockwood CM, Hoffman JM, West SG, Sheets V. A comparison of methods to test mediation and other intervening variable effects. *Psychol. Methods* 7(1), 83–104 (2002).
22. Houseman EA, Molitor J, Marsit CJ. Reference-free cell mixture adjustments in analysis of DNA methylation data. *Bioinformatics* 30(10), 1431–1439 (2014).
23. Robins JM, Greenland S. Identifiability and exchangeability for direct and indirect effects. *Epidemiology* 3(2), 143–155 (1992).
24. Rubin DB. Bayesian inference for causal effects: the role of randomization. *Ann. Statist.* 6(1), 34–58 (1978).
25. VanderWeele T, Vansteelandt S. Conceptual issues concerning mediation, interventions and composition. *Stat. Interface* 2, 457–468 (2009).
26. Vanderweele TJ. A unification of mediation and interaction. *Epidemiology* 25(5), 749–761 (2014).
27. Huang Y-T. Joint significance tests for mediation effects of socioeconomic adversity on adiposity via epigenetics. *Ann. Statist.* 1–24 (2018).
28. McLean CY, Bristor D, Hiller M *et al.* GREAT improves functional interpretation of cis-regulatory regions. *Nat. Biotechnol.* 28(5), 495–501 (2010).
29. Han R, Wang X, Bachovchin W, Zukowska Z, Osborn JW. Inhibition of dipeptidyl peptidase 8/9 impairs preadipocyte differentiation. *Sci. Rep.* 5(12348), 1–11 (2015).
30. Berndt J, Kovacs P, Ruschke K *et al.* Fatty acid synthase gene expression in human adipose tissue: association with obesity and Type 2 diabetes. *Diabetologia* 50(7), 1472–1480 (2007).
31. Gracia A, Elcoroaristizabal X, Fernández-Quintela A *et al.* Fatty acid synthase methylation levels in adipose tissue: effects of an obesogenic diet and phenol compounds. *Genes Nutr.* 9(4), 29 (2014).
32. Edwards DR, Handsley MM, Pennington CJ. The ADAM metalloproteinases. *Mol. Aspects Med.* 29(5), 258–289 (2008).
33. Ponnuchamy B, Khalil RA. Role of ADAMs in endothelial cell permeability: cadherin shedding and leukocyte rolling. *Circ. Res.* 102(10), 1139–1142 (2008).
34. Schierding W, O'Sullivan JM. Connecting SNPs in diabetes: a spatial analysis of meta-GWAS loci. *Front. Endocrinol.* 6, 102 (2015).
35. Tsurutani Y, Fujimoto M, Takemoto M *et al.* The roles of transforming growth factor-Î^2 and Smad3 signaling in adipocyte differentiation and obesity. *Biochem. Biophys. Res. Comm.* 407(1), 68–73 (2011).
36. Yadav H, Quijano C, Kamaraju AK *et al.* Protection from obesity and diabetes by blockade of TGF-β/Smad3 signaling. *Cell Metab.* 14(1), 67–79 (2011).
37. Wehner M, Clemens PR, Engel AG, Kilimann MW. Human muscle glycogenosis due to phosphorylase kinase deficiency associated with a nonsense mutation in the muscle isoform of the α subunit. *Hum. Mol. Genet.* 3(11), 1983–1987 (1994).
38. Jiang H, Westerterp M, Wang C, Zhu Y, Ai D. Macrophage mTORC1 disruption reduces inflammation and insulin resistance in obese mice. *Diabetologia* 57(11), 2393–2404 (2014).
39. Lee PL, Tang Y, Li H, Guertin DA. Raptor/mTORC1 loss in adipocytes causes progressive lipodystrophy and fatty liver disease. *Mol. Metabol.* 5(6), 422–432 (2016).

40. Loucks EB, Huang Y-T, Agha G *et al.* Epigenetic mediators between childhood socioeconomic disadvantage and mid-life body mass index: the New England Family Study. *Psychosom. Med.* 78(9), 1053–1065 (2016).

•• **Demonstrates association of early life socioeconomic indicators and DNA methylation with adulthood BMI, also using a two-stage mediation approach.**

41. Haim Y, Blüher M, Konrad D *et al.* ASK1 (MAP3K5) is transcriptionally upregulated by E2F1 in adipose tissue in obesity, molecularly defining a human dys-metabolic obese phenotype. *Mol. Metabol.* 6(7), 725–736 (2017).

42. Desideri E, Vegliante R, Cardaci S, Nepravishta R, Paci M, Ciriolo MR. MAPK14/p38α-dependent modulation of glucose metabolism affects ROS levels and autophagy during starvation. *Autophagy* 10(9), 1652–1665 (2014).

43. Meng W, Veluchamy A, Hébert HL, Campbell A, Colhoun HM, Palmer CNA. A genome-wide association study suggests that MAPK14 is associated with diabetic foot ulcers. *Br. J. Dermatol.* 93, 215–217 (2017).

44. Waterworth DM, Li L, Scott R *et al.* A low-frequency variant in MAPK14 provides mechanistic evidence of a link with myeloperoxidase: a prognostic cardiovascular risk marker. *J. Am. Heart Assoc.* doi:10.1161/JAHA.114.001074 (2014).

45. Zhang Y, Nguyen T, Tang P *et al.* Regulation of adipose tissue inflammation and insulin resistance by MAPK phosphatase 5. *J. Biol. Chem.* 290(24), 14875–14883 (2015).

46. Bost F, Aouadi M, Caron L, Binétruy B. The role of MAPKs in adipocyte differentiation and obesity. *Biochimie* 87(1), 51–56 (2005).

47. Weaver ICG, Cervoni N, Champagne FA *et al.* Epigenetic programming by maternal behavior. *Nat. Neurosci.* 7(8), 847–854 (2004).

48. Champagne FA. Interplay between social experiences and the genome: epigenetic consequences for behavior. *Adv. Genet.* 77, 33–57 (2012).

49. Champagne FA, Curley JP. How social experiences influence the brain. *Curr. Opin. Neurobiol.* 15(6), 704–709 (2005).

50. López-Jaramillo P, Silva SY, Rodríguez-Salamanca N, Duràn A, Mosquera W, Castillo V. Are nutrition-induced epigenetic changes the link between socioeconomic pathology and cardiovascular diseases? *Am. J. Ther.* 15(4), 362–372 (2008).

51. Hoffmann A, Spengler D. DNA memories of early social life. *Neuroscience* 264, 64–75 (2014).

52. Bick J, Naumova O, Hunter S *et al.* Childhood adversity and DNA methylation of genes involved in the hypothalamus–pituitary–adrenal axis and immune system: whole-genome and candidate-gene associations. *Dev. Psychopathol.* 24(4), 1417–1425 (2012).

53. Miller GE, Chen E, Fok AK *et al.* Low early-life social class leaves a biological residue manifested by decreased glucocorticoid and increased proinflammatory signaling. *Proc. Natl Acad. Sci. USA* 106(34), 14716–14721 (2009).

54. Groom A, Potter C, Swan DC *et al.* Postnatal growth and DNA methylation are associated with differential gene expression of the TACSTD2 gene and childhood fat mass. *Diabetes* 61(2), 391–400 (2012).

55. Godfrey KM, Sheppard A, Gluckman PD *et al.* Epigenetic gene promoter methylation at birth is associated with child's later adiposity. *Diabetes* 60(5), 1528–1534 (2011).

56. Kuehnen P, Mischke M, Wiegand S *et al.* An Alu element-associated hypermethylation variant of the POMC gene is associated with childhood obesity. *PLoS Genet.* 8(3), e1002543 (2012).

57. Relton CL, Groom A, St Pourcain B *et al.* DNA methylation patterns in cord blood DNA and body size in childhood. *PLoS ONE* 7(3), e31821 (2012).

58. Almén MS, Jacobsson JA, Moschonis G *et al.* Genome wide analysis reveals association of a FTO gene variant with epigenetic changes. *Genomics* 99(3), 132–137 (2012).

59. Zhao J, Goldberg J, Vaccarino V. Promoter methylation of serotonin transporter gene is associated with obesity measures: a monozygotic twin study. *Int. J. Obes.* 37(1), 140–145 (2013).

60. Goni L, Milagro FI, Cuervo M, Martínez JA. Single-nucleotide polymorphisms and DNA methylation markers associated with central obesity and regulation of body weight. *Nutr. Rev.* 72(11), 673–690 (2014).

61. Zhang FF, Cardarelli R, Carroll J *et al.* Significant differences in global genomic DNA methylation by gender and race/ethnicity in peripheral blood. *Epigenetics* 6(5), 623–629 (2011).

62. Miller GE, Chen E, Parker KJ. Psychological stress in childhood and susceptibility to the chronic diseases of aging: moving toward a model of behavioral and biological mechanisms. *Psychol. Bull.* 137(6), 959–997 (2011).

63. Danese A, Tan M. Childhood maltreatment and obesity: systematic review and meta-analysis. *Mol. Psychiatry* 19(5), 544–554 (2013).

64. Slopen N, Kubzansky LD, McLaughlin KA, Koenen KC. Childhood adversity and inflammatory processes in youth: a prospective study. *Psychoneuroendocrinology* 38(2), 188–200 (2013).

65. Nazmi A, Oliveira IO, Horta BL, Gigante DP, Victora CG. Lifecourse socioeconomic trajectories and C-reactive protein levels in young adults: findings from a Brazilian birth cohort. *Soc. Sci. Med.* 70(8), 1229–1236 (2010).

66. Loucks EB, Pilote L, Lynch JW *et al.* Life course socioeconomic position is associated with inflammatory markers: the Framingham Offspring Study. *Soc. Sci. Med.* 71(1), 187–195 (2010).

67. Pollitt RA, Kaufman JS, Rose KM, Diez-Roux AV, Zeng D, Heiss G. Early-life and adult socioeconomic status and inflammatory risk markers in adulthood. *Eur. J. Epidemiol.* 22(1), 55–66 (2007).

68. Danese A, Moffitt TE, Harrington H *et al.* Adverse childhood experiences and adult risk factors for age-related disease: depression, inflammation, and clustering of metabolic risk markers. *Arch. Pediatr. Adolesc. Med.* 163(12), 1135–1143 (2009).
69. Slopen N, Lewis TT, Gruenewald TL *et al.* Early life adversity and inflammation in African Americans and whites in the midlife in the United States survey. *Psychosom. Med.* 72(7), 694–701 (2010).
70. Slopen N, Loucks EB, Appleton AA *et al.* Early origins of inflammation: an examination of prenatal and childhood social adversity in a prospective cohort study. *Psychoneuroendocrinology* 51, 403–413 (2015).
71. Gershon NB, High PC. Epigenetics and child abuse: modern-day darwinism – the miraculous ability of the human genome to adapt, and then adapt again. *Am. J. Med. Genet. C Semin. Med. Genet.* 169(4), 353–360 (2015).
72. Heim C, Newport DJ, Mletzko T, Miller AH, Nemeroff CB. The link between childhood trauma and depression: insights from HPA axis studies in humans. *Psychoneuroendocrinology* 33(6), 693–710 (2008).
73. Bell CG, Teschendorff AE, Rakyan VK, Maxwell AP, Beck S, Savage DA. Genome-wide DNA methylation analysis for diabetic nephropathy in Type 1 diabetes mellitus. *BMC Med. Genomics* 3(1), 33 (2010).
74. Xu Z, Bolick SCE, DeRoo LA, Weinberg CR, Sandler DP, Taylor JA. Epigenome-wide association study of breast cancer using prospectively collected sister study samples. *J. Natl Cancer Inst.* 105(10), 694–700 (2013).
75. Cordoba R, Sanchez-Beato M, Herreros B *et al.* Two distinct molecular subtypes of chronic lymphocytic leukemia give new insights on the pathogenesis of the disease and identify novel therapeutic targets. *Leuk. Lymph.* 57(1), 134–142 (2015).
76. Rubicz R, Zhao S, Geybels M *et al.* DNA methylation profiles in African American prostate cancer patients in relation to disease progression. *Genomics* doi:10.1016/j.ygeno.2016.02.004 (2016).
77. van Dam PA, van Dam P-JHH, Rolfo C *et al. In silico* pathway analysis in cervical carcinoma reveals potential new targets for treatment. *Oncotarget* 7(3), 2780–2795 (2016).
78. Houtepen LC, Vinkers CH, Carrillo-Roa T *et al.* Genome-wide DNA methylation levels and altered cortisol stress reactivity following childhood trauma in humans. *Nat. Commun.* 7, 10967 (2016).
79. Moffatt MF, Kabesch M, Liang L *et al.* Genetic variants regulating ORMDL3 expression contribute to the risk of childhood asthma. *Nature* 448(7152), 470–473 (2007).
80. Amos CI, Wu X, Broderick P *et al.* Genome-wide association scan of tag SNPs identifies a susceptibility locus for lung cancer at 15q25.1. *Nat. Genet.* 40(5), 616–622 (2008).